Search for top-quark decays to real W bosons at the Fermilab Tevatron collider

H. Baer
Physics Department, Florida State University, Tallahassee, Florida 32306

V. Barger
Physics Department, University of Wisconsin, Madison, Wisconsin 53706

R. J. N. Phillips
Rutherford Appleton Laboratory, Chilton, Didcot, Oxon, England
(Received 23 January 1989)

We propose ways in which eventual signals from heavy-top-quark decays into on-shell or nearly-on-shell W bosons may be discriminated more sharply from background at the Fermilab Tevatron $\bar{p}p$ collider. For single-lepton $\bar{t}t$ signals, the principal background from direct W production cannot be eliminated by acceptance cuts alone, but the signal/background ratio can be greatly increased by requiring a high jet multiplicity n. Top-quark signals can be detected and m_t can be measured via enhancements in the single-lepton event rates at high n, or via a peak in the invariant mass of the three hardest jets at high n. A $\bar{t}t$ signal can be extracted up to $m_t = 150$ GeV (180 GeV) from selected data with $n \geq 3$ ($n \geq 4$) jets. For two-lepton $\bar{t}t$ signals, the principal standard-model backgrounds from $\bar{b}b, \bar{c}c$ and Drell-Yan dilepton production can all be removed by cuts. The remaining backgrounds from direct W^+W^- and Drell-Yan $\bar{\tau}\tau$ production can be suppressed to a level well below the $\bar{t}t$ signals, for the whole of the mass range up to $m_t = 200$ GeV allowed for the standard model. Eventual $\bar{t}t$ signals can be confirmed by characteristic dynamical distributions. An integrated luminosity of 10 pb^{-1} (100 pb^{-1}) would be enough to detect top quarks up to $m_t = 120$ GeV (200 GeV).

I. INTRODUCTION

To produce and identify particles containing the top quark t remains one of the outstanding challenges of the standard model (SM). The top quark is required theoretically to cancel triangle anomalies,[1] to explain the suppression of neutral-current B-meson decays,[2] and to account for the observed value of the $e^+e^- \to b\bar{b}$ forward-backward jet asymmetry[3]. Its mass m_t is an important parameter, unknown but constrained by various data and theoretical considerations. The absence of $e^+e^- \to \bar{t}t$ signals[4] gives a direct limit $m_t > 27.4$ GeV; top searches at the CERN $\bar{p}p$ collider[5] give $m_t > 41$ GeV. In the minimal SM with radiative corrections, consistency of different data with a common set of parameters gives the upper bound $m_t \lesssim 150$–200 GeV (depending on the unknown Higgs-boson mass).[6] Arguments based on renormalization-group fixed points[7] favor values of order $m_t \sim 100$–200 GeV (though strictly speaking these are upper limits). Arguments based on observed $B_d^0 - \bar{B}_d^0$ oscillations suggest[8] a lower bound $m_t > 40$–50 GeV. Indirect measurements of Γ_Z/Γ_W have suggested[9] an upper bound of order $m_t \lesssim 60$–70 GeV, but the present uncertainties in structure functions needed to extract Γ_Z/Γ_W preclude a firm bound at present. Any value in the range $41 \lesssim m_t \lesssim 200$ GeV may therefore be expected at present. Experiments already running on the $\bar{p}p$ colliders at CERN ($\sqrt{s} = 630$ GeV) and Fermilab ($\sqrt{s} = 1.8$ TeV) will soon have new results probing the lower part of this mass range.

If $m_t < M_W$, the SM semileptonic decays $t \to b\bar{l}\nu$ ($l = e$ or μ) offer promising ways to tag top-quark events. Experimental signatures based on these decays and on the decays of associated $\bar{t}$ or $\bar{b}$ jets have been extensively studied and are well understood; backgrounds from $\bar{c}c$ and $\bar{b}b$ production can be controlled (extensive references may be found in Ref. 10). For such a "light" top quark, the problem of how to extract a signal from background is essentially solved. In the present paper we concentrate attention on the possibility that t is heavy, $m_t \gtrsim M_W$. In this eventuality top-quark decay proceeds via $t \to b + W^+$ into real on-shell W bosons (or slightly off-shell bosons with similar decay properties); subsequent leptonic W decays $W^- \to \bar{l}\nu$ are still a valid tag for top events, but a new background from $p\bar{p} \to W$+jets is now relevant and proves more difficult to separate than the $b\bar{b}$ and $c\bar{c}$ backgrounds. Several studies[10–13] have already been made of heavy-top production at the Fermilab Tevatron that illustrate these difficulties and suggest some other ways to identify and clarify the top signal. It is our purpose here to propose new ways to refine the signals of a heavy-top quark and suppress the backgrounds.

In Sec. II we examine and discuss the general features of $\bar{p}p \to \bar{t}tX \to \bar{b}bW^-W^+X$ events. Their most promising signatures are based on either (i) an isolated lepton plus missing p_T plus jets, or (ii) two leptons plus missing p_T. We also consider the principal sources of backgrounds, which are $\bar{p}p \to W$+jets, $\bar{p}p \to \gamma^*$ or Z+jets, $\bar{p}p \to \bar{b}bX$ (or $\bar{c}cX$), and $\bar{p}p \to W^+W^-X$ events. Their general features differ from those of top events; a variety of experimental cuts are suggested to suppress these backgrounds. In Secs. III and IV we present realistic calculations of $\bar{t}t$ signals and backgrounds, for both one-lepton and two-lepton signatures, and demonstrate the efficiency

of our chosen cuts. We summarize our conclusions in Sec. V.

II. HEAVY-TOP-QUARK SIGNATURES

A. Top production and decay

At a $\bar{p}p$ collider the production of heavy quarks Q proceeds in lowest order α_s^2 by the $2\rightarrow 2$ QCD subprocesses

$$\bar{q}q\rightarrow\bar{Q}Q,\quad gg\rightarrow\bar{Q}Q\ , \tag{1}$$

where q and g denote light quarks and gluons. In order α_s^3 various $2\rightarrow 3$ subprocesses contribute also:

$$\bar{q}q\rightarrow\bar{Q}Qg,\quad gg\rightarrow\bar{Q}Qg,\quad gq\rightarrow\bar{Q}Qq,\quad g\bar{q}\rightarrow\bar{Q}Q\bar{q}\ . \tag{2}$$

For the case of top quarks ($Q=t$) with $m_t > M_W$, there are no significant electroweak production processes. QCD total-cross-section formulas for heavy-quark production, complete through order α_s^3, have recently been given.[14] Figure 1 shows the predicted values for a range of top-quark masses at $\sqrt{s}=1.8$ and 2.0 TeV, the present and future Fermilab Tevatron operating energies. Our calculations use Duke-Owens 1 parton distributions[15] evolved up to the scale $Q^2=\hat{s}$, the subprocess c.m. energy squared; there is an overall uncertainty of some tens of percent in such calculations, from the uncertainty in choice of parton distributions and scale.

It is instructive to briefly consider event rates at the Tevatron. Assuming an integrated luminosity of 10 pb^{-1} after a year or so of running, Fig. 1 indicates that about 400 $\bar{t}t$ events would be produced if $m_t=120$ GeV. Allowing a factor of a few percent for branching fractions and experimental acceptance (see below), this implies of order 10 detected events, and probably marks the upper limit for exploring m_t in the immediate future. Nevertheless, we shall extend our discussion to include higher values of m_t, bearing in mind possible future Tevatron upgrades that might provide integrated luminosity of order 100 pb^{-1} or more. Our considerations apply also to possible pp collisions for which the principal $gg\rightarrow\bar{t}t(g)$ channels are identical.

In the present work we assume $m_t \gtrsim M_W$; t decays are then dominated by on-shell W bosons (or nearly on-shell W with similar properties), which decay in turn to pairs of leptons or quarks:

$$t\rightarrow bW^+,\quad W^+\rightarrow\bar{e}\nu,\bar{\mu}\nu,\bar{\tau}\nu,\bar{q}q'\ . \tag{3}$$

Since all QCD production channels lead to $\bar{t}t$ pairs, top events are almost entirely of the form

$$\bar{p}p\rightarrow\bar{t}tX\rightarrow\bar{b}bW^-W^+X\ , \tag{4}$$

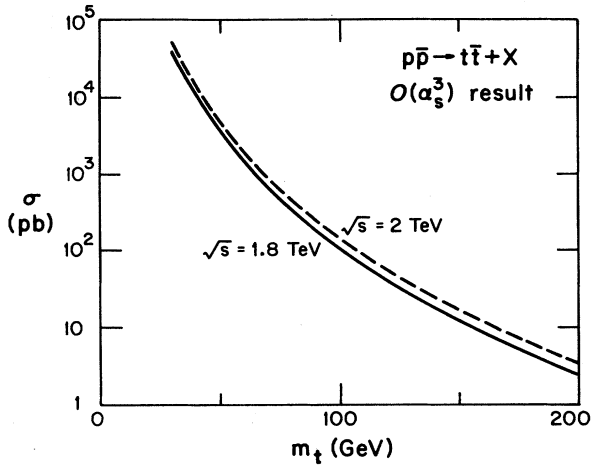

FIG. 1. Total $\bar{p}p\rightarrow\bar{t}tX$ production cross section vs m_t at $\sqrt{s}=1.8$ and 2.0 TeV, calculated from the $O(\alpha_s^3)$ formulas (Ref. 14) with Duke-Owens distributions (Ref. 15) at scale $Q^2=\hat{s}$.

which is most remarkable for the appearance of W^-W^+ pairs (although the $\bar{b}$ and b jets are also potentially very distinctive). The cleanest W signature in $\bar{p}p$ collisions[16] is a high-p_T isolated lepton $l=e$, μ, or τ, plus large missing-p_T (henceforth denoted $\not{p}_T$) in the opposite hemisphere, with transverse mass[17,18] $m_T(l,\not{p}_T)$ distribution peaked near M_W. The most frequent W signature, however, is a pair of high-p_T jets with invariant mass near M_W, arising with about 60% branching fraction from $W\rightarrow\bar{q}q'$ modes (after allowing for semileptonic $\bar{q}$ or q' decay[19]). Hitherto jet energy resolution has restricted the usefulness of this $W\rightarrow$two-jet signature,[20] but the latest upgraded detectors are expected to be able to exploit it.

The first essential components of a top event signature are therefore *two* W signatures, either (i) two high-mass pairs of jets, or (ii) one high-mass jet pair, plus one high-p_T lepton with high transverse mass $m_T(l,\not{p}_T)$, or (iii) two high-p_T leptons with high $\not{p}_T$, with possible additional jets in all cases from $\bar{b}$ or b or QCD radiation.

Before we analyze these classes of signature, it is instructive to examine the kinematics of heavy-top decays. The basic quarks and leptons are the same as those appearing in light top three-body decays via virtual W, but the sequential two-body structure of Eq. (3) imposes new sharp peaks in the $\bar{l}\nu$ and $\bar{q}q'$ invariant masses, plus Jacobian peaks in all transverse momenta and the transverse mass $m_T(\bar{l},\nu)$. Also, in common with three-body modes, the $b\bar{q}q'$ invariant mass and the cluster transverse mass[21] $m_T(b\bar{l},\nu)$ peak near m_t. Specifically,

$m(\bar{q}q')\simeq M_W$	Breit-Wigner peak,	
$p_T(\bar{l}),p_T(\nu),p_T(\bar{q}),p_T(q')$	peaks near $\frac{1}{2}M_W$	in the W rest frame
$m_T(\bar{l},\nu)$	peak near M_W	in the W rest frame
$p_T(b),p_T(W)$	peaks near $\lambda^{1/2}(m_t^2,m_b^2,M_W^2)/(2m_t)$	in the t rest frame
$m_T(b\bar{l},\nu)$	peak near m_t	in the t rest frame
$m(b\bar{q}q')\simeq m_t$	Breit-Wigner peak	

where $\lambda(a,b,c)=a^2+b^2+c^2-2ab-2bc-2ca$. In the laboratory frame, the QCD production mechanisms give substantial p_T to $\bar{t},t$ and hence to W^-,W^+, with $\langle p_T(t)\rangle \sim \langle p_T(W)\rangle \sim \frac{1}{2}m_t$. In boosting to the laboratory frame, the p_T peaks of their decay products are smeared but the m_T peaks are almost unchanged.[18] Hence for $m_t=90$ GeV, the b jet has p_T peaking at 7 GeV, smeared around this value in the laboratory frame (suppression of b momentum for m_t near M_W is a direct consequence of the sequential two-body decay structure). It is therefore inconspicuous compared to the $\bar{q}$ and q' jets from W, which have p_T peaking at 40 GeV in the W rest frame, smeared around this value in the laboratory. For $m_t=110$ GeV the b jet is much more conspicuous, with p_T peaking near 25 GeV. For $m_t=130$ GeV the Jacobian peak of $p_T(b)$ is at 40 GeV, making b jets as prominent as the quark jets from W decay.

B. All-jet signatures

The SM branching fraction for $W\to\bar{q}q'$ decay is about 68% (for $m_t>M_W$) so about 45% of all $\bar{t}t$ production leads to hadronic states

$$\bar{t}t\to\bar{b}bW^+W^-\to\bar{b}b(q_1\bar{q}_2)(\bar{q}_3q_4) \tag{5}$$

typically giving rise to four high-p_T jets with $m(j_1j_2)\simeq m(j_3j_4)\simeq M_W$. At the Tevatron the cross section for this channel falls from about 160 pb for $m_t=80$ GeV to about 1 pb for $m_t=200$ GeV. There is, however, a severe background from QCD multijet production:[22] e.g., the calculated cross section[23] for four jets with $p_T>30$ GeV and $|\eta|<3.5$ is 12 nb.

It may be possible to separate the $\bar{t}t\to\bar{b}bW^+W^-$ signal from QCD background by stringent application of the invariant-mass constraints and by exploiting the additional $\bar{b}$ and b jets. This possibility depends sensitively on detector resolution, however; we postpone a discussion until detector performance at the Tevatron becomes better known. Microvertex detectors could also aid in identifying the $\bar{b},b$ jets.

C. One-lepton-plus-jets signatures

The SM branching fraction for $W\to e\nu$ decay is 10.8% (for $m_t>M_W$); similarly for $W\to\mu\nu$. Hence about 29% of heavy top events have one such W decay, giving

$$\bar{t}t\to\bar{b}bW^+W^-\to l^\pm+\not{p}_T+(n\le 4)\text{ jets} \tag{6}$$

with $l=e$ or μ, plus possible additional jets from QCD radiation. The lepton has a high probability to be isolated, i.e., to have little hadronic energy emitted in a small cone about the lepton momentum direction.

About 5% of $\bar{t}t$ events lead to the same final configuration Eq. (6) via $W\to\tau\nu\to l\nu\nu\nu$ decays; they are indistinguishable from direct $W\to e\nu,\mu\nu$ decays except for softer p_T and m_T spectra. In addition, about 9% of $t\bar{t}$ events lead via $W\to\tau\bar{\nu}\to\bar{\nu}\nu\bar{q}q'$ to final states similar to Eq. (6), except that $l^\pm$ is now replaced by a narrow low-multiplicity τ jet. Such $W\to(\tau\text{ jet})+\not{p}_T$ decays have been successfully identified in single-W events with a missing-p_T trigger,[24] but we shall not pursue them further in this section.

The principal backgrounds come from $\bar{b}b$ or $\bar{c}c$ production (with semileptonic decay of a b or c quark) and from direct W production (with $W\to l\nu$ decay); additional QCD jets may be radiated in both cases. We require dynamical quantities that distinguish the $\bar{t}t$ signal.

(i) Lepton isolation. In $H\to hl\nu$ semileptonic decay of a heavy-flavor hadron H, if the lepton has $p_T(l)\gg m_H$, kinematics constrain the hadronic decay products h to be emitted mostly close to the lepton momentum direction. Hence if we require $p_T(l)\gg m_b$ and impose a stringent upper limit on hadronic energy emitted close to l, we can suppress the background from $\bar{b}b$ and $\bar{c}c$ production (see, e.g., Ref. 10), albeit at some cost to the $\bar{t}t$ signal. But the direct W+jets background cannot be suppressed in this way.

(ii) Lepton p_T. The $b\bar{b}$ ($c\bar{c}$) backgrounds peak at low p_T, leptons from $W\to l\nu$ peak around $p_T\sim 40$ GeV. Requiring a high minimum $p_T(l)$ discriminates against $\bar{b}b$ ($\bar{c}c$) but not against direct W production.

(iii) Missing p_T. Just as for charged-lepton p_T, requiring high $\not{p}_T$ discriminates against $\bar{b}b$ ($\bar{c}c$) but not against direct W production.

(iv) Lepton-$\not{p}_T$ correlations. For a parent W with $p_T(W)\ll M_W$ the lepton and missing neutrino are correlated back to back:

$$p_T(l)\simeq\not{p}_T,\quad \Delta\phi(l,\not{p}_T)\simeq 180^\circ\,, \tag{7}$$

where $\Delta\phi$ denotes azimuthal-angle difference. These correlations are observed for direct $W\to l\nu$ events.[16] They will be smeared by $p_T(W)$ for $\bar{t}t\to W^-W^+$ events and for direct W+multijet events; they are not expected for $\bar{b}b$ ($\bar{c}c$) events.

(v) Leptonic transverse mass. The transverse mass $m_T(l,\not{p}_T)$ defined by[17]

$$m_T^2(l,\not{p}_T)=[p_T(l)+\not{p}_T]^2-[\mathbf{p}_T(l)+\not{\mathbf{p}}_T]^2 \tag{8}$$

also exploits the lepton-neutrino correlations and has an almost unsmeared[18] Jacobian peak at $m_T\simeq 80$ GeV. It discriminates more sharply against $\bar{b}b$ and $\bar{c}c$ than either (ii) or (iii), and has long been recognized[21,25,26] as a useful signature for lighter top quarks. But for $m_t>M_W+m_b$ the $\bar{t}t$ signal has the same shape of $m_T(l,\not{p}_T)$ distribution as the direct W background.

(vi) Two hardest jets. In events such as Eq. (6) there is a large probability (reducing as m_t increases) that the two jets with largest p_T come from the hadronic $W\to\bar{q}q'$ decay and therefore have invariant mass near m_W. A peak in $m(j_1j_2)$ near M_W therefore distinguishes $\bar{t}t$ from $\bar{b}b$ ($\bar{c}c$) or direct W events, but the latter nonetheless contribute a high continuum background.

(vii) Three hardest jets. There is also substantial probability that the three jets with highest p_T in Eq. (6) come from $t\to bW^+\to b\bar{q}q'$ decay (or similar $\bar{t}$ decay) and therefore have invariant mass near m_t. A peak in $m(j_1j_2j_3)$ distinguishes $\bar{t}t$ from all backgrounds and measures m_t.

(viii) Cluster transverse mass. The transverse mass of a

cluster of particles c, combined with $\not{p}_T$ from a missing neutrino ν, is defined by[21]

$$m_T^2(c,\not{p}_T)=\left[\left[p_{cT}^2+m_c^2\right]^{1/2}+\not{p}_T\right]^2-(\mathbf{p}_{cT}+\not{\mathbf{p}}_T)^2 . \quad (9)$$

This m_T has a Jacobian peak at the invariant mass of the $(c+\nu)$ system. Since the lepton and $\not{p}_T$ in Eq. (6) come from a $t\to bW\to bl\nu$ decay sequence, the transverse mass $m_T(bl,\not{p}_T)$ of the cluster $c=bl$ peaks at m_t. The problem is to choose which (if any) of the jets comes from the associated b quark. If we sum over all possible choices, the m_T distribution will have a peak at m_T plus a continuum from the "wrong" choices. The optimum choice depends on m_t. W+jets and $\bar{b}b$ ($\bar{c}c$) backgrounds have no comparable cluster-m_T peaks.

(ix) Summed transverse energy. Heavy $\bar{t}t$ events are characterized by big energy release, leading to large $\sum E_T$ measured in the detector calorimeters. Our calculations show that $\sum E_T$ is useful in discriminating against W+jets and $\bar{b}b$ ($\bar{c}c$) backgrounds, which have softer distributions than $\bar{t}t$ when $m_T > M_W$.

(x) W/Z event ratio. Heavy $\bar{t}t$ events contribute to the inclusive $W\to e\nu$ event rate but not to the inclusive $Z\to ee$ event rate (defined by the ee invariant mass peak). Hence the $(W\to e\nu)/(Z\to ee)$ event ratio provides in principle a measurement of the $\bar{t}t$ signal. The $\bar{t}t$ correction to this rate is about 3.7% for $m_t=70$ GeV and 1.5% for $m_t=90$ GeV.

(xi) Jet multiplicity. Heavy $\bar{t}t$ events have typically two or more jets whereas direct W production gives mostly zero or one jet. This difference can be exploited to enhance various top signals.[25]

D. Two-lepton signatures

In the SM about 10.5% of all heavy $\bar{t}t$ events have two $W\to l\nu$ leptonic decays where now l denotes e or μ or τ:

$$\bar{t}t\to\bar{b}bW^-W^+\to\bar{b}bl_1^-l_2^++\not{p}_T . \quad (10)$$

Here both leptons have high probability to be isolated; jets can arise from $\bar{b}$ or b or additional QCD radiation. We stress the importance of including the $W\to\tau\nu$ decay modes if possible; without them, the ee, $e\mu$, and $\mu\mu$ modes alone have only 4.7% branching fraction. Subsequent $\tau\to e\nu\nu,\mu\nu\nu$ decays contribute events indistinguishable from direct $W\to e\nu,\mu\nu$ contributions (apart from softer p_T spectra); the remaining $\tau\to\nu qq'$ decays give narrow isolated low-multiplicity jets that can be directly identified.[24] The principal backgrounds are the Drell-Yan process $\bar{p}p\to(\gamma^*$ or $Z)\to e^-e^+,\mu^-\mu^+,\tau^-\tau^+$ and hadronic $\bar{b}b$ ($\bar{c}c$) production with two semileptonic b or c decays. However, the direct electroweak production of W^+W^- pairs also becomes non-negligible for $m_t > 150$ GeV; this background shares all the characteristic properties of the heavy $\bar{t}t$ signal except for the accompanying $\bar{b}$ and b jets.

(i) Lepton flavors. The $\bar{t}t$ signal gives e^-e^+, $e^-\mu^+$, μ^-e^+, and $\mu^-\mu^+$ pairs with equal probability; so does the $\bar{b}b$ ($\bar{c}c$) background; but the Drell-Yan process gives mostly e^-e^+ and $\mu^-\mu^+$ plus small $e\mu$ contributions via $\tau^+\tau^-$ decays. Let us use the symbol τ_h to denote hadronic τ decays (one-prong plus three-prong modes have 64% branching fraction) and disregard the relatively soft e and μ coming from secondary decays $\tau\to e,\mu$ or $b\to c\to e,\mu$ or $t\to b\to e,\mu$ as a first approximation (the third assumption is only reasonable for m_t near M_W). Then $\bar{t}t$ decay gives equal $e^-\tau_h^+$, τ_h^-, $\tau_h^-e^+$, $\mu^-\tau_h^+$, and $\tau_h^-\mu^+$ rates at 64% of the e^-e^+ signal; the Drell-Yan process gives equal but negligible rates; $\bar{b}b$ gives equal rates at about 13% of the e^-e^+ rate since $(b\to\tau)/(b\to e)$ suppression is about $\frac{1}{5}$; $\bar{c}c$ gives zero rates. Finally, $\tau_h^-\tau_h^+$ states are produced by $\bar{t}t$ or the Drell-Yan process at about 40% of the e^-e^+ rate, by $\bar{b}b$ at about 1.6% of the e^-e^+ rate, by $\bar{c}c$ not at all. These numbers illustrate how τ_h modes can both amplify the dilepton signal and give cross-checks on signal purity.

(ii) Lepton isolation and p_T. The high p_T and isolation of the $\bar{t}t$ leptons help to distinguish them from $\bar{b}b$ ($\bar{c}c$) leptons, as in Sec. IIC, but not from Z-decay or W^+W^- backgrounds.

(iii) Missing p_T. $\not{p}_T$ is typically much larger for the $\bar{t}t$ signal than for the principal backgrounds. The Drell-Yan contributions have little $\not{p}_T$ (arising through hadronic measurement uncertainties), except in channels with $\tau\to e,\mu$ decay.

(iv) Dilepton angular correlation. The azimuthal-angle difference $\Delta\phi(l_1^-,l_2^+)$ between the two leptons is a powerful discriminator of backgrounds.[27] Drell-Yan or $\bar{b}b$ ($\bar{c}c$) contributions are strongly peaked at $\Delta\phi(l_1^-,l_2^+)\sim 0$ and 180°, with very little in between. The $\Delta\phi\sim 0°$ peak comes from low-mass Drell-Yan pairs and from cascade b decays ($b\to cl_1\nu$, $c\to sl_2\nu$); the $\Delta\phi\sim 180°$ peak comes from non-cascade-associated pairs ($b\to l_1X_1$, $\bar{b}\to l_2X_2$) and from $Z\to l_1l_2$. Signals from $t\bar{t}$ events are broadly distributed across the azimuthal angular range.

(v) Dilepton invariant mass. Drell-Yan dileptons from $\bar{q}q\to Z\to l_1^-l_2^+$ have invariant mass $m(l_1l_2)\simeq M_Z$; those from $\bar{q}q\to\gamma^*\to l_1^-l_2^+$ are peaked at low mass. Cascade b-decay backgrounds have $m(l_1l_2)<m_b$. Invariant-mass cuts can suppress such backgrounds.

(vi) Dilepton–missing-p_T correlations. The dilepton analogs of the lepton-neutrino correlations of Eq. (7) are

$$p_T(l\bar{l})\simeq\not{p}_T,\quad \Delta\phi(l\bar{l},\not{p}_T)\simeq 180° , \quad (11)$$

where $\mathbf{p}_T(ll)=\mathbf{p}_T(l_1)+\mathbf{p}_T(l_2)$ is the vector sum of the two charged-lepton momenta and $\Delta\phi$ denotes the azimuthal-angle difference between it and $\mathbf{p}_T$. Equation (11) applies for $l=e$, μ, or τ_h. It is true in the approximation that $p_T(W^+W^-)=0$, which is most nearly applicable when $m_t\simeq M_W+m_b$. Hence for the $\bar{t}t$ signals, $d\sigma/d\Delta\phi$ peaks at 180°; also the distributions versus $p_T(ll)-\not{p}_T$ and versus $|\mathbf{p}_T(ll)+\not{\mathbf{p}}_T|$ both peak at zero. Only the backgrounds from the Drell-Yan process $Z\to\tau\tau\to l_1l_2\not{p}_T$ and direct W^+W^- production have the same correlations [in the approximation that $p_T(Z)=0=p_T(WW)$]. Low-mass $\gamma^*\to\tau\bar{\tau}\to l_1\bar{l}_2\not{p}_T$ and cascade b decays give $\Delta\phi\simeq 0°$ and no correlations in magnitude of p_T; noncascade $\bar{b}b$ ($\bar{c}c$) decays give $\Delta\phi\simeq 0°$ or 180° but no correlation in magnitudes.

(vii) Dilepton–missing-p_T transverse mass. The cluster transverse mass[21] $m_T(l_1\bar{l}_2,\not{p}_T)$, defined as in Eq. (9) for the cluster $c=l_1+l_2$ combined with $\not{p}_T$, also exploits the lepton-neutrino correlations. The $\bar{t}t$ signal has distinctively large values, typically in the range m_t to $2m_t$, reflecting the large energy release in the decay chain. For $Z\to ee,\mu\mu$ events m_T peaks at M_Z; for $Z\to\tau\tau\to l_1 l_2\not{p}_T$ events $m_T\lesssim M_Z$. For b-cascade decays $m_T<m_b$ (apart from $\not{p}_T$ smearing). Noncascade $\bar{b}b$ ($\bar{c}c$) contributions are also peaked at small m_T values, but a region of small m_T is suppressed by setting minimum thresholds for $p_T(l)$ and $\not{p}_T$.

III. CALCULATIONS

We calculate the $\bar{p}p\to\bar{t}tX$ total cross section from the $O(\alpha_s^3)$ formulas[14] as described in Sec. II A. We calculate the differential distributions by Monte Carlo methods from the $2\to3$ subprocesses of Eq. (2), which give the correct dependence on $p_T(\bar{t}t)$ at large values, using the formulas of Ref. 28. The divergence at $p_T(\bar{t}t)=0$ is removed by a multiplicative Gaussian cutoff factor $F(p_T)=1-\exp(-p_T^2/A^2)$ with the parameter A adjusted to reproduce the correct total $\bar{t}tX$ cross section. This is a truncated-shower approximation.[10,29]

We assume that the top quarks form top-flavored hadrons with essentially the same mass m_t and the same four-momentum; we treat the subsequent decays of Eq. (3) as free-quark decays, neglecting polarization correlations between $\bar{t}$ and t (which give at most small effects[30]). For $m_t>120$ GeV, t quarks would be expected mostly to decay *before* hadronization,[30] but within our approximations the results are the same. We include the full $t\to b\to c\to s$ decay cascade.

For the heavy-quark backgrounds, we calculate $\bar{p}p\to\bar{b}bX,\bar{c}cX$ production similarly to the $\bar{t}tX$ case above. We assume that b and c quarks fragment into B and D hadrons, respectively, according to the model of Peterson *et al.*[31] (calculated in the production subprocess rest frame with parameter $\epsilon=0.5/m^2$, where m is the quark mass in GeV). We choose values $m_b=m_B=5.2$ GeV and $m_c=m_D=1.87$ GeV. The b quark from $t\to bW$ decay is treated similarly.

The decays of B and D hadrons are approximated by free-quark decays $b\to cxy$ and $c\to sxy$. The fragmentation of the c quark produced in B decay is known experimentally to be very hard[32] (apparently the energy release is too small for the arguments of Ref. 31 to apply), so we approximate the $c\to D$ fragmentation function by $D(z)=\delta(1-z)$ in this case, with $z=p_D/p_c$ the usual momentum fraction. The decays of τ leptons are represented by $\tau\to\nu xy$ with $V-A$ matrix elements ($xy=e\bar{\nu},\mu\bar{\nu},d\bar{u}$), using the observed branching fractions for leptonic and hadronic modes.

The cross sections for $V=W,Z,\gamma^*$ production include the usual factor of $K=1+\frac{8}{9}\pi\alpha_s(M_V)$; the distributions for $\bar{p}p\to V+$jets are obtained from the QCD shower Monte Carlo model of Gottschalk,[33] which agrees with experiment at $\sqrt{s}=630$ GeV and with perturbative calculations.[34] We calculate W^+W^- production from the formulas of Ref. 35, neglecting explicit jet production in this case; from shower calculations for one produced vector boson of mass $2M_W$, we estimate that 80% (16%) of direct WW events have $n=0$ ($n=1$) jets, with our jet criteria below. All our QCD calculations are performed at the parton level. Final quarks or gluons with sufficiently high p_T (see criteria below) are interpreted as jets, with $E_T(\text{jet})=p_T(\text{parton})$. Jets with $\Delta R<0.7$ are coalesced, with ΔR being defined by

$$\Delta R=[(\Delta\eta)^2+(\Delta\phi)^2]^{1/2}\ , \tag{12}$$

where $\eta=\ln\cot(\theta/2)$ is pseudorapidity, and θ is a polar angle.

Jet E_T is subject to measurement uncertainty; we approximate this by a random Gaussian correction to each jet, with mean zero and standard deviation $0.8\sqrt{E_T}$. E_T uncertainties also contribute to an error in $\not{p}_T$, which is essentially a random Gaussian correction to each of the (x,y) transverse components of $\not{p}_T$, with mean zero and standard deviation $0.4(\sum E_T)^{1/2}$, where $\sum E_T$ is the sum of all E_T in the event.[36] Here $\sum E_T$ is the sum of jets from the hard-scattering process in question, plus a contribution from the underlying soft event. We represent the latter by a random variable, parametrized numerically to reproduce the observed $\sum E_T$ distribution in minimum-bias events[37] at $\sqrt{s}=540$ GeV, scaled up by a factor of 1.5 for the observed ratio of $\sum E_T$ between minimum-bias and hard-scattering events such as W production[16] and by a further factor of 1.3 for the rise in central multiplicity $dn/d\eta$ between $\sqrt{s}=540$ GeV and 1.8 TeV (Ref. 38).

We define the following acceptance criteria for counting jets:

$$E_T(\text{jet})>15\text{ GeV},\quad |\eta(\text{jet})|<2.5\ . \tag{13}$$

IV. RESULTS

A. Single-lepton signals

We concentrate attention on events with one isolated lepton (e or μ) plus missing p_T, satisfying the following lepton and $\not{p}_T$ cuts:

(a) $p_T(e,\mu,\tau_h)>20$ GeV.

(b) $|\eta(e)|<3.0$, $|\eta(\mu)|<0.76$, $|\eta(\tau_h)|<1.0$.

(c) $\not{p}_T>20$ GeV.

(d) Isolation: $\sum_c E_T<3$ GeV in cone $\Delta R<0.4$ about lepton momentum.

The η cuts above correspond approximately to the acceptance of the Collider Detector at Fermilab (CDF). The p_T and isolation cuts are to reduce backgrounds. To illustrate the size of the signals and backgrounds remaining after these cuts, Table I lists the cross sections in the electron channel, separated according to the number n of accompanying jets.

Table I shows that the $\bar{b}b,\bar{c}c$ backgrounds are enormously suppressed by the acceptance cuts. These cuts do not suppress the electroweak W production background; on the contrary, they are precisely the kind of cuts normally invoked to select a $W\to e\nu$ signal.[16] However, the $\bar{t}t/(W+\bar{b}b)$=signal/background ratio is greatly

TABLE I. Cross sections in pb for $e\nu$ events from W and heavy-quark production, and for $Z\to\bar{e}e$ events, at $\sqrt{s}=1.8$ TeV after acceptance cuts (a)–(d) of Sec. IV A. Results are given for top-quark masses 70, . . . , 190 GeV; $\bar{c}c$ contributions are negligible after cuts.

Channel	$n\geq 0$ jets	$n\geq 1$ jets	$n\geq 2$ jets	$n\geq 3$ jets
$W\to e\nu$	1730	260	47	5
$Z\to ee$	154	26	5	0.7
$\bar{b}b$	6	6	1.4	0
$\bar{t}t(70)$	45	40	27	10
$\bar{t}t(90)$	24	20	15	4
$\bar{t}t(110)$	9	8	7	4
$\bar{t}t(130)$	4	4	3	2
$\bar{t}t(150)$	1.8	1.8	1.7	1.2
$\bar{t}t(170)$	0.9	0.9	0.9	0.6
$\bar{t}t(190)$	0.5	0.5	0.5	0.4

enhanced by requiring high jet multiplicity n. Indeed, we may hope to detect $\bar{t}t$ signals directly in this way, as illustrated in Figs. 2 and 3 for the case $m_t=70$ GeV.

Figure 2 shows a histogram of the event fractions $\sigma(\text{“}W\text{”}, n, \text{or more jets})/\sigma(\text{all “}W\text{”})$, where “$W$” denotes $e\nu$ events passing the acceptance cuts (a)–(d). For $n=0$ this fraction is 1 by definition; for $n=1$ it is dominated by direct $W\to e\nu$ events; for $n=2$ and $n=3$ the $\bar{t}t$ contribution gives substantial enhancements above the values expected from W+jets shower calculations.[33] The shaded areas show the enhancements. Figure 3 gives a histogram of the event ratios $\sigma(\text{“}W\text{”}, n, \text{or more jets})/\sigma(Z\to ee, n, \text{or more jets})$, derived from Table I. For $n=0$ or 1 this ratio is dominated by direct W,Z production; however, a 70-GeV top quark enhances the ratio by a factor of 1.6 for $n=2$ and by a factor of 3 for $n=3$. Structure function uncertainties in the $W+n$ jet and $Z+n$ jet calculations cancel in these ratios. K-factor uncertainties[39] plausibly cancel in the W/Z ratio. In principle a $\bar{t}t$ contribution can be detected, without prior removal of the electroweak W background, simply from the shapes of these histograms.[25] In each case the $n=0$ and $n=1$ data serve to confirm (or normalize) the $W+n$ jet background calculation; the $n\geq 2$ and $n\geq 3$ data contain the $\bar{t}t$ signals; the size of these signals determines m_t.

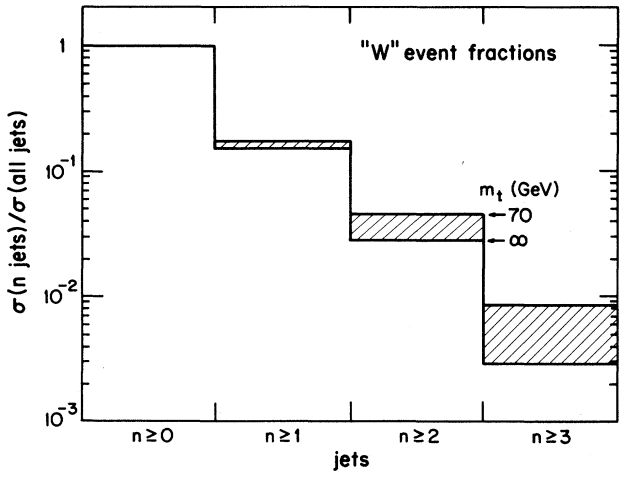

FIG. 2. Histogram of the event fractions $\sigma(\text{“}W\text{”}, n \text{ or more jets})/\sigma(\text{all “}W\text{”})$ for $n=0,1,2,3$; lower histogram is for the case $m_t=\infty$ (no $\bar{t}t$ signal), upper histogram is for $m_t=70$ GeV. The shaded areas show the $\bar{t}t(70)$ signals.

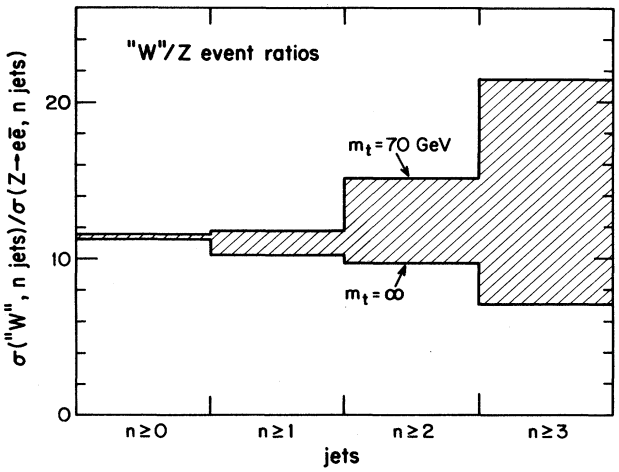

FIG. 3. Histogram of the even ratios $\sigma(\text{“}W\text{”}, n, \text{or more jets})/\sigma(Z\to ee, n, \text{or more jets})$ for $n=0,1,2,3$; lower histogram is the $m_t=\infty$ (no $\bar{t}t$ signal), upper histogram is for $m_t=70$ GeV. The shaded areas show the $\bar{t}t(70)$ signals.

In order to suppress the electroweak W background somewhat, we henceforth require $n\geq 2$ jets and an additional transverse-mass cut, as discussed in Sec. II C:

(e) Number of jets $n\geq 2$.

(f) 25 GeV $< m_T(l,\not{p}_T) <$ 100 GeV.

With these cuts, the W background still dominates over the t-quark signal, as can be seen in the $\sum E_T$ distribution of Fig. 4; to improve the signal to background we impose an additional cut:

(g) $\sum E_T > 210$ GeV.

For $m_t\sim M_W$ the two jets with highest p_T (labeled j_1 and j_2) almost always come from W decay and have invariant mass near M_W. Figure 5 shows the distributions

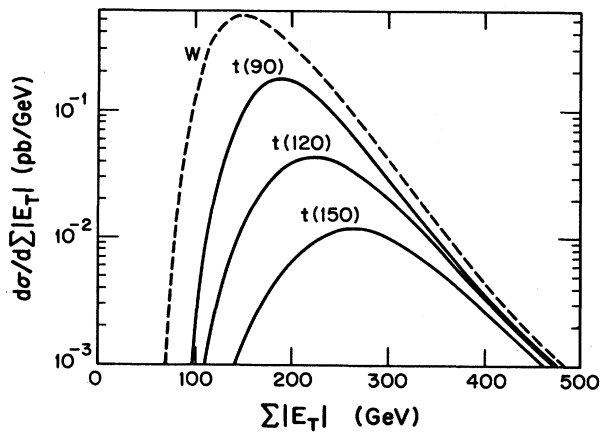

FIG. 4. Distribution vs summed transverse energy of hadrons $\sum E_T$ for single-lepton events satisfying the cuts (a)–(f) of Sec. IV A, summed over e and μ events.

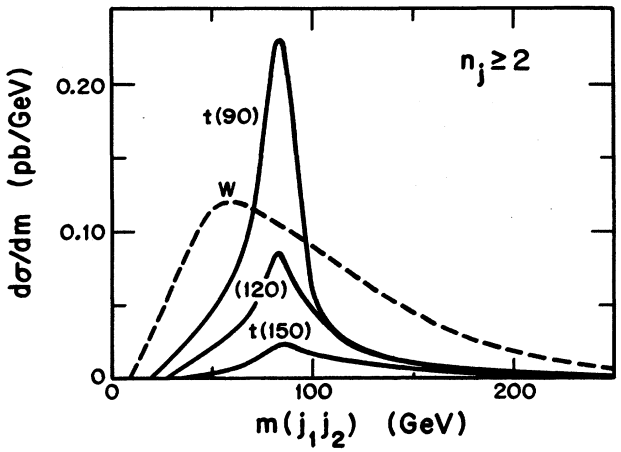

FIG. 5. Distribution vs the invariant mass $m(j_1 j_2)$ of the two highest-p_T jets in lepton plus ($n \geq 2$) jet events, satisfying cuts (a)–(g) of Sec. IV A, summed over e and μ cases.

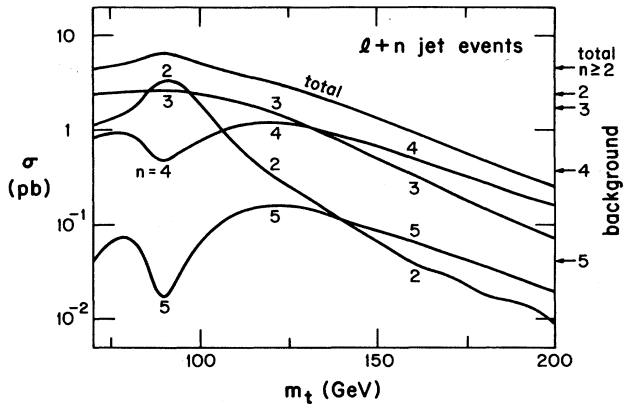

FIG. 6. Topological cross sections for $\bar{t}t \to$ lepton plus ($n \geq 2$) jet events satisfying cuts (a)–(h) of Sec. IV A, vs m_t. The case $l = e, \mu$ are summed. Contributions from $n = 2,3,4,5$ jet events, their total, and backgrounds are shown.

of $\bar{t}t$ signal and the various backgrounds versus $m(j_1 j_2)$ with cuts (a)–(g); the signal peaks at $m(j_1 j_2) = M_W$ as expected, but this peak is smeared by contamination from b jets for $m_t \gg M_W$. We therefore also impose an additional requirement:

(h) $|m(j_a j_b) - M_W| < 15$ GeV, for some pair of jets in the event, which is satisfied by most $\bar{t}t \to WW$ events.

Table II compares the cross sections of the $\bar{t}t$ signal and various backgrounds (summed over e and μ channels), first with basic cuts (a)–(d), then with additional cuts (e)–(h). The suppression of the $\bar{t}t$ signal for $m_t < 90$ GeV occurs because the cuts (f)–(h) are not optimal in this region; we have retained them here simply for compactness of presentation.

Figure 6 gives the cross section for $\bar{t}t$ events satisfying the cuts (a)–(h) vs m_t, showing also the separate contributions from n-jet topologies for $n = 2,3,4,5$. The peak and dips for $n = 2,4,5$ near $m_t = M_W + m_b$ are due to kinematic suppression of decay b jets in this region (Sec. II A). Background contributions are indicated by arrows on the right-hand side. For higher values on the m_t range, a better signal/background ratio is obtained in the higher jet multiplicities; the $l+4$ jets channel exceeds background for $m_t < 175$ GeV.

Figure 7 shows the cross-section dependence on $p_T(W) = |\mathbf{p}_T(l) + \not{\mathbf{p}}_T|$ for $\bar{t}t$ signal and W background events with $n \geq 2$ or 3 jets, satisfying cuts (a)–(h). Figure 8 illustrates the corresponding cross-section dependence on transverse mass $m_T(l, \not{p}_T)$, omitting the m_T cut in this case so that its effect can be seen and also showing the effects of omitting the isolation cut. This shows how the large $\bar{b}b$, $\bar{c}c$ backgrounds are first considerably reduced by the m_T cut and finally removed by the isolation requirement; the suppression does not rely too heavily on any single cut.

To extract m_t we consider the invariant mass $m(j_1 j_2 j_3)$ of the *three* jets with highest p_T. Figure 9(a) shows the distribution of signal and background versus $m(j_1 j_2 j_3)$ in ($n \geq 3$) jet events. A plot of this quantity measures m_t when $100 < m_t < 150$ GeV; in this range the signal is above background and a hard b jet is frequently among the three hardest jets. For very heavy top it is desirable to select higher jet multiplicity, as remarked above. Figure 9(b) shows the distributions versus $m(j_1 j_2 j_3)$ for ($n \geq 4$) jet events. Assuming an eventual integrated luminosity of 100 pb^{-1}, the selection of these $n \geq 3$ and $n \geq 4$ data samples would provide a clear $\bar{t}t$ signal up to about $m_t = 180$ GeV; it might be possible to go still further by selecting $n \geq 5$.

TABLE II. Cross sections in pb for $e\nu$ plus $\mu\nu$ events at $\sqrt{s} = 1.8$ TeV with alternative sets of acceptance cuts, either (a)–(d) or (a)–(h). Results are given for top-quark signals with $m_t = 70, \ldots, 200$ GeV and for W, $\bar{b}b$, and $\bar{c}c$ backgrounds.

Channel	Cuts (a)–(d)	Cuts (a)–(h)
$\bar{t}t(70)$	63.0	4.4
$\bar{t}t(80)$	46.0	5.1
$\bar{t}t(90)$	35.0	6.5
$\bar{t}t(100)$	22.0	5.1
$\bar{t}t(110)$	13.0	4.0
$\bar{t}t(120)$	8.8	3.3
$\bar{t}t(130)$	5.9	2.5
$\bar{t}t(140)$	4.0	1.8
$\bar{t}t(150)$	2.8	1.3
$\bar{t}t(160)$	2.0	0.95
$\bar{t}t(170)$	1.4	0.67
$\bar{t}t(180)$	1.1	0.48
$\bar{t}t(190)$	0.77	0.35
$\bar{t}t(200)$	0.58	0.26
W	2435.0	4.4
$\bar{b}b$	7.1	0
$\bar{c}c$	0.008	0

B. Two-lepton signals

We select $\bar{p}p \to l_1^- l_2^+ \not{p}_T$ events with two oppositely charged isolated leptons, satisfying the following cuts:

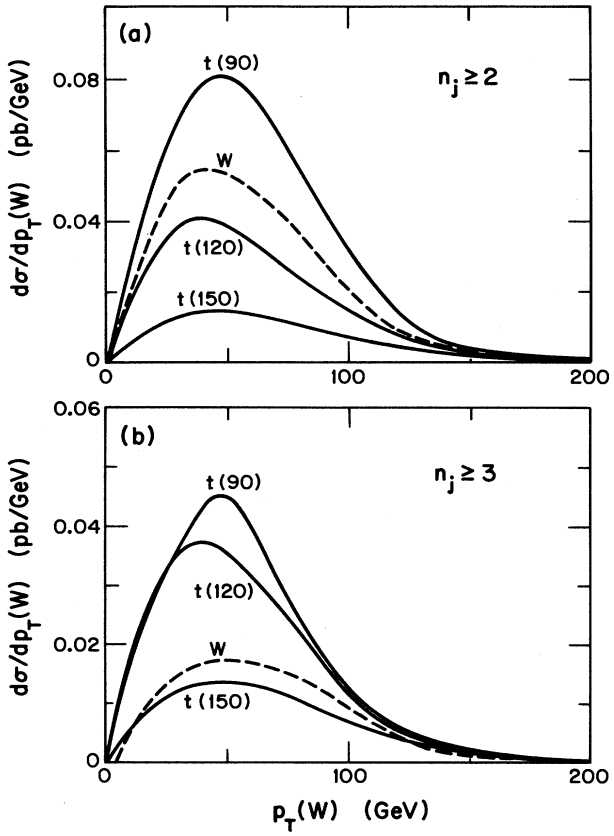

FIG. 7. Signal and background distributions vs $p_T(W)=|\mathbf{p}_T(l)+\not{\mathbf{p}}_T|$ for single-lepton events satisfying full cuts of Sec. IV A. (summed over $l=e,\mu$ cases) for (a) $n \geq 2$ jets, (b) $n \geq 3$ jets.

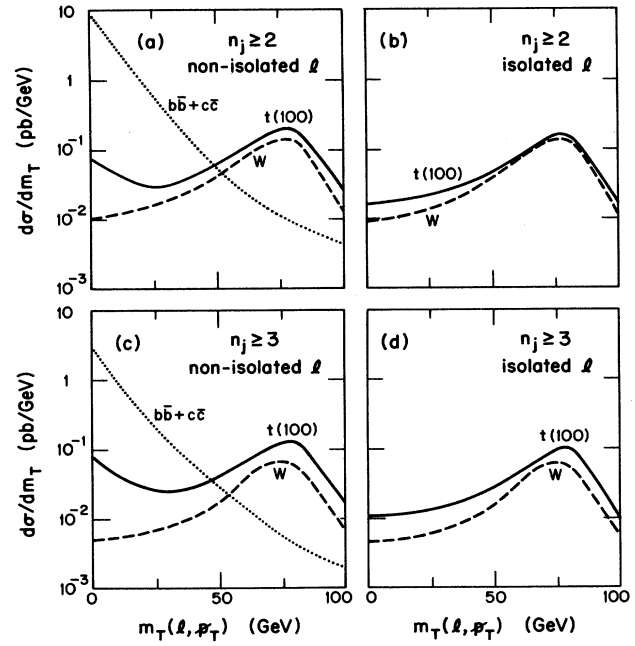

FIG. 8. Signal and background distributions vs transverse mass $m_T(l,\not{p}_T)$ for single-lepton events satisfying the full cuts of Sec. IV A excepting the m_T cut, both with and without the isolation cut: (a) jet multiplicity $n \geq 2$, nonisolated; (b) $n \geq 2$ isolated, (c) $n \geq 3$ nonisolated; (d) $n \geq 3$ isolated.

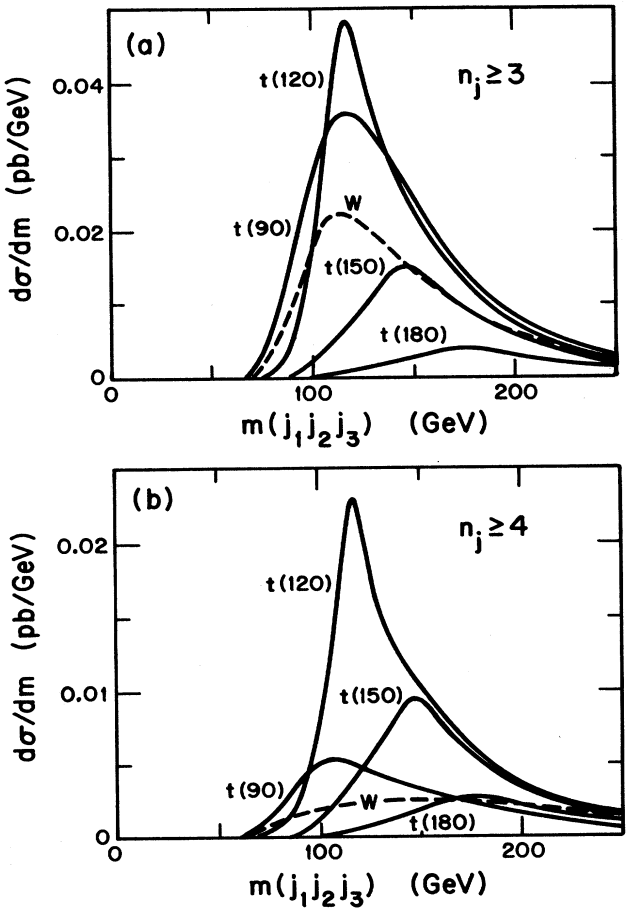

FIG. 9. Distribution vs the invariant mass $m(j_1j_2j_3)$ of the three jets with highest p_T in single-lepton events with cuts (a)–(h) of Sec. IV A (summing e and μ modes) for (a) $n \geq 3$ jets, (b) $n \geq 4$ jets.

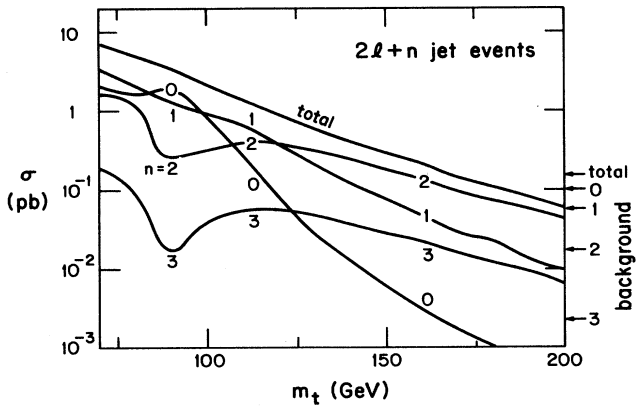

FIG. 10. Total and topological cross sections for $\bar{t}t \rightarrow$dilepton plus n-jet events satisfying the cuts (a)–(e) of Sec. IV B, vs m_t, summed over all electron and muon channels. Contributions from $n=0,1,2,3$ jet events, their total, and backgrounds are shown.

(a) $p_T(e,\mu,\tau_h) > 15$ GeV.
(b) $|\eta(e)| < 3.0$, $|\eta(\mu)| < 0.76$, $|\eta(\tau_h)| < 1.0$.
(c) $\not{p}_T > 20$ GeV.
(d) isolation: $\sum_c E_T < 3$ GeV in cone $\Delta R < 0.4$ about lepton momentum.

These are similar to those in Sec. IV A except that the $\not{p}_T(l)$ cut is a little less severe. In addition we impose a cut on the azimuthal-angle difference $\Delta\phi(l_1 l_2)$ between the leptons:

(e) $30° < \Delta\phi(l_1 l_2) < 150°$.

Together with the isolation cut (d), this effectively suppresses[27] the large background from $\bar{b}b$ ($\bar{c}c$) production, leaving a rather clean $\bar{t}t$ signal with small backgrounds from WW and $Z,\gamma^* \to \bar{\tau}\tau$ production. Table III compares the cross sections of the $\bar{t}t$ signal and the various backgrounds (summed over ee, $e\mu$, and $\mu\mu$ channels) first with basic cuts (a)–(c) alone, then with the additional isolation and azimuthal cuts (d) and (e). Henceforth we use the full cuts (a)–(e). (Using rather similar cuts, we have previously presented some heavy $\bar{t}t$ dilepton results in Refs. 40 and 41.)

Figure 10 shows the total and topological cross sections for $n=0$, 1, 2, or 3 jets versus m_t. The reduction in the mean number of jets near $m_t = M_W + m_b$ is due to the suppression of the decay b and $\bar{b}$ momenta in this region, described in Sec. II A. The mass m_t can, in principle, be extracted from the total event rate; the topological cross sections provide a number of independent cross-checks on m_t. If we require $n \geq 2$ jets, the background from $Z,\gamma^* \to \bar{\tau}\tau$ and WW production is reduced to below 0.02 pb; this is substantially smaller than the $\bar{t}t$ signal right up to $m_t = 200$ GeV, the upper end of the SM range (Sec. I). With an eventual integrated luminosity of 100 pb^{-1} or more, a $\bar{t}t$ dilepton signal would be detectable through the full mass range.

For further discussion in the present paper, we shall allow any number of jets ($n \geq 0$); this is quite sufficient for the mass range of most immediate interest up to $m_t = 120$ GeV, where a luminosity of 10 pb^{-1} would yield a significant $\bar{t}t$ dilepton signal dominating comfortably over background. (We note, however, that in the following figures a cut $n \geq 2$ would leave the $t\bar{t}$ curves essentially unchanged apart from a small reduction in normalization, for $m_t > 120$ GeV).

Figure 11(a) illustrates the cross-section dependence on $p_T(l_{\text{hard}}) = \max\{p_T(l_1), p_T(l_2)\}$, the transverse momentum of the harder lepton. Figure 11(b) gives the distribution versus maximum lepton laboratory energy $E(l_{\text{fast}}) = \max\{E(l_1), E(l_2)\}$. Figure 12(a) shows the dependence on the dilepton transverse momentum $p_T(ll) = |\mathbf{p}_T(l_1) + \mathbf{p}_T(l_2)|$ and Figure 12(b) gives the behavior versus missing p_T (omitting the $\not{p}_T$ cut in this figure). Figures 13(a) and 13(b) give the dependences on the dilepton invariant mass $m(l_1 l_2)$ and azimuthal

TABLE III. Cross sections in pb for ee plus $\mu\mu$ plus $e\mu$ dilepton events at $\sqrt{s} = 1.8$ TeV with alternative cuts (a)–(c) or (a)–(e). Results are given for $\bar{t}t$ signals with $m_t = 70, \ldots, 200$ GeV and for various backgrounds.

Channel	Cuts (a)–(c)	Cuts (a)–(e)
$\bar{t}t(70)$	12.0	7.3
$\bar{t}t(80)$	9.1	5.0
$\bar{t}t(90)$	6.3	3.5
$\bar{t}t(100)$	4.1	2.1
$\bar{t}t(110)$	3.0	1.4
$\bar{t}t(120)$	2.3	0.91
$\bar{t}t(130)$	1.8	0.60
$\bar{t}t(140)$	1.4	0.42
$\bar{t}t(150)$	1.1	0.29
$\bar{t}t(160)$	0.91	0.22
$\bar{t}t(170)$	0.72	0.14
$\bar{t}t(180)$	0.58	0.11
$\bar{t}t(190)$	0.47	0.08
$\bar{t}t(200)$	0.37	0.06
$\bar{b}b$	65.0	0
$\bar{c}c$	9.2	0
$Z,\gamma^* \to \bar{\tau}\tau$	0.14	0.055
$Z,\gamma^* \to ee,\mu\mu$	0.007	0
WW	0.17	0.12

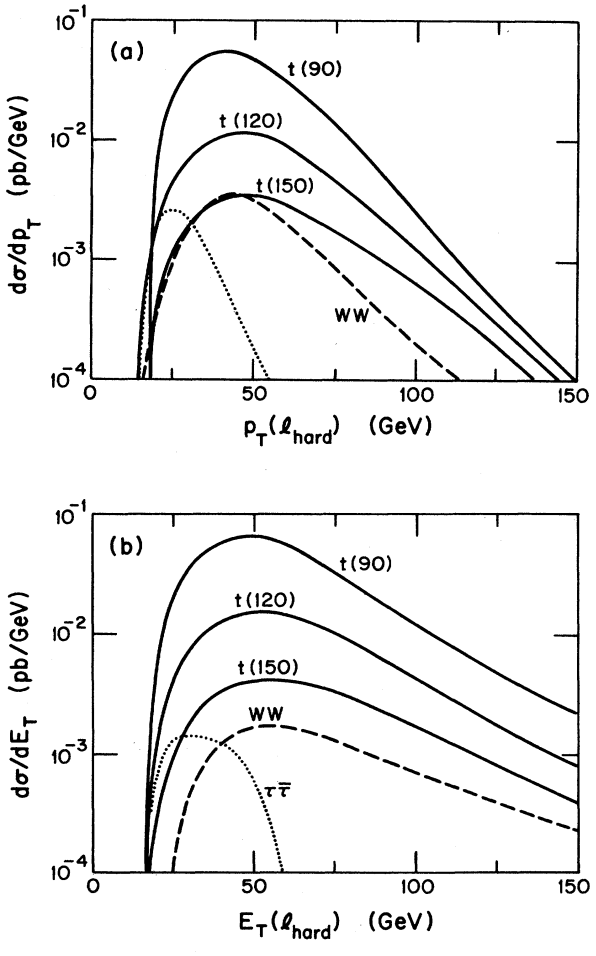

FIG. 11. Distributions of dilepton events satisfying the full cuts of Sec. IV B (summing ee, $\mu\mu$, $e\mu$ modes) vs (a) $p_T(l_{\text{hard}}) = \max\{p_T(l_1), p_T(l_2)\}$, (b) $E(l_{\text{fast}}) = \max\{E(l_1), E(l_2)\}$.

difference $\Delta\phi(l_1 l_2)$. In many of the above dynamical distributions, the $\bar{t}t$ signal behaves quite differently from the $Z,\gamma^* \to \bar{\tau}\tau$ background, showing that the latter at least can be easily separated.

Figure 13(c) shows the predicted distribution versus the cluster transverse mass $m_T(ll,\not{p}_T)$. This too can be used to determine m_t. Figure 14 illustrates the dilepton-$\not{p}_T$ correlations discussed in Sec. II D, showing the distributions versus the azimuthal difference $\Delta\phi(ll,\not{p}_T)$ and versus the scalar transverse-momentum difference $\Delta p_T = [p_T(ll) - \not{p}_T]$. For values of m_t near $M_W + m_b$ there are narrow peaks at $\Delta\phi \simeq 180°$ and $\Delta p_T \simeq 0$ as expected; for other values of m_t these peaks are progressively broadened. The shapes of these peaks can be used to help in determining m_t. In Fig. 14 the WW background has been calculated from the lowest-order diagrams,[35] for which $p_T(WW)=0$ and the distributions are idealized δ functions shown as narrow boxes; in practice we expect the distributions to be smeared into narrow peaks with shapes similar to the $\bar{t}t(90)$ curves.

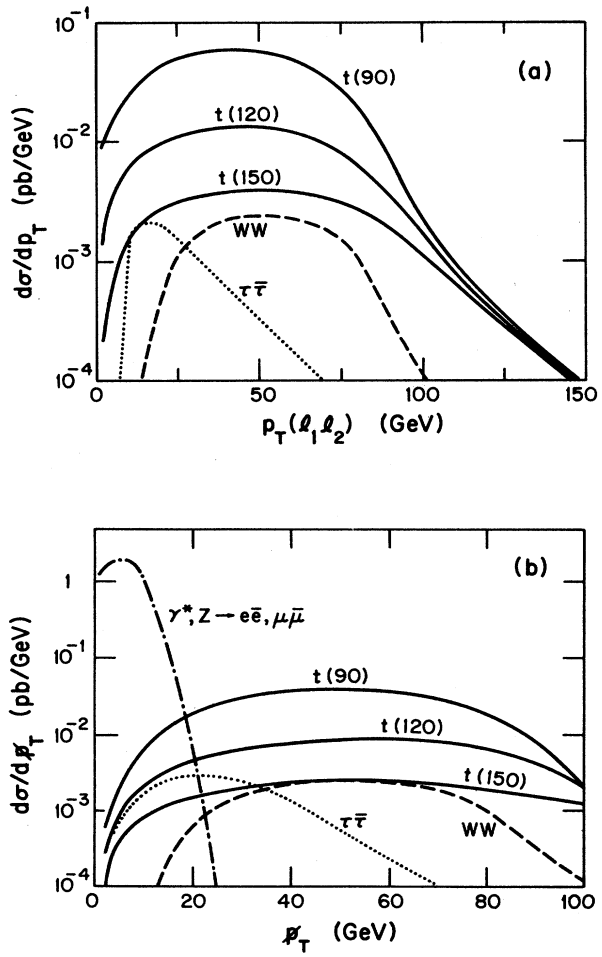

FIG. 12. Distributions of dilepton events satisfying the full cuts of Sec. IV B (summing ee, $\mu\mu$, $e\mu$ modes) vs (a) dilepton transverse momentum $p_T(l_1 l_2) = |\mathbf{p}_T(l_1) + \mathbf{p}_T(l_2)|$, (b) missing p_T, omitting the p_T cut here.

It is important to know the relative rates in different dilepton channels; their ratios offer further cross-checks on a $\bar{t}t$ mechanism as discussed in Sec. II D. For the case $m_t = 90$ GeV we calculate the following cross sections in picobarns:

$$\sigma(ee)=1.45,\quad \sigma(\mu\mu)=0.45,\quad \sigma(\tau_h\tau_h)=0.45\ ,$$

$$\sigma(\mu\tau_h)=0.90,\quad \sigma(e\tau_h)=1.6,\quad \sigma(e\mu)=1.6\ .$$

The ratios vary rather weakly with m_t.

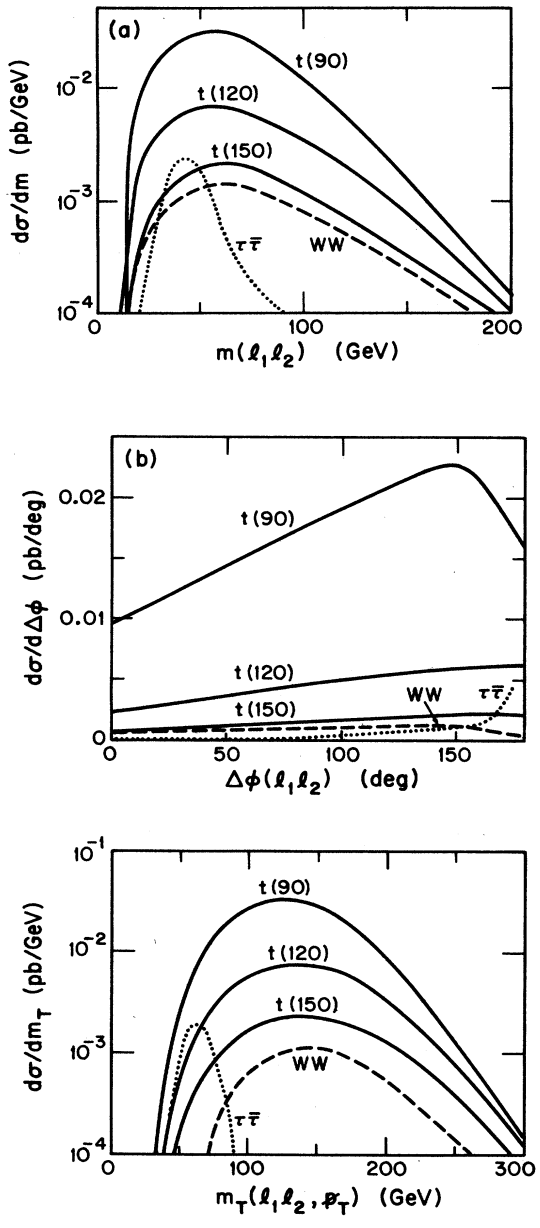

FIG. 13. Distributions of dilepton events satisfying the full cuts of Sec. IV B (summing ee, $\mu\mu$, $e\mu$ modes: (a) dilepton invariant mass $m(l_1 l_2)$; (b) dilepton azimuthal-angle difference $\Delta\phi(l_1 l_2)$, omitting the $\Delta\phi$ cut; (c) cluster transverse mass $m_T(l_1 l_2, \not{p}_T)$.

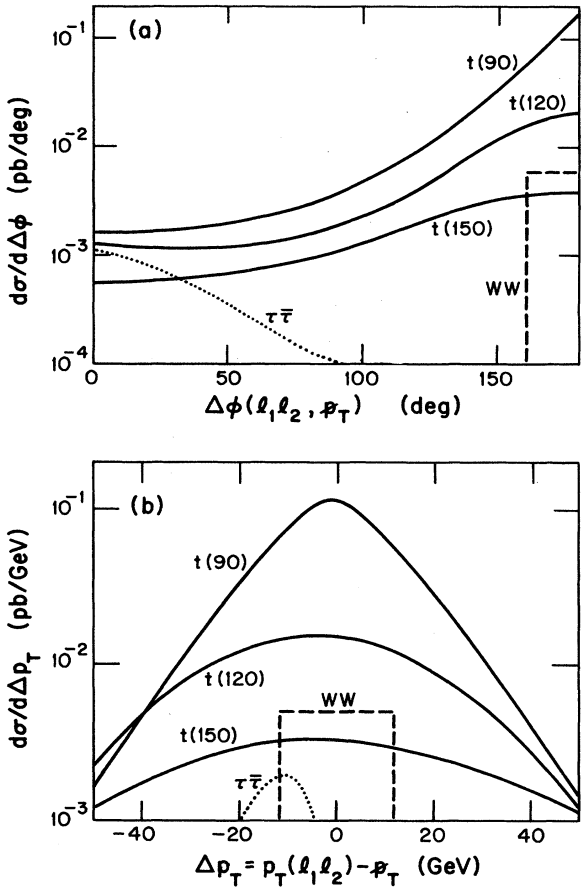

FIG. 14. Dilepton-$\not{p}_T$ correlations in $\bar{t}t \to l_1^- l_2^+ \not{p}_T$ events with full cuts: (a) distribution vs azimuthal difference $\Delta\phi(l_1 l_2, \not{p}_T)$; (b) distribution vs scalar transverse-momentum difference $\Delta p_T = p_T(l_1 l_2) - \not{p}_T$.

V. SUMMARY

For single-lepton signals, our results show the following.

(i) $\bar{b}b, \bar{c}c$ backgrounds can be removed as usual by $p_T(l), \not{p}_T$ and lepton isolation cuts.

(ii) Electroweak W background cannot be eliminated, but can be minimized by selecting high jet multiplicity n and high $\sum E_T$.

(iii) $\bar{t}t$ signals can be extracted directly from the shape of the histograms for $\sigma(\text{"}W\text{"}, n, \text{or more jets})/\sigma(\text{all "}W\text{"})$ or for $\sigma(\text{"}W\text{"}, n, \text{or more jets})/\sigma(Z \to ee, n, \text{or more jets})$, without prior removal of the W background; the size of the signals determines m_t.

(iv) $\bar{t}t$ signals can be found as peaks in the invariant mass of the three hardest jets, in events with $n \geq 3$ jets; for very heavy t it is better to require $n \geq 4$ jets; the position of this peak determines m_t.

(v) For an eventual luminosity of 100 pb^{-1}, these techniques can detect $\bar{t}t$ signals up to $m_t = 180$ GeV.

For two-lepton signals, our results show the following.

(vi) The principal standard-model backgrounds from $\bar{b}b, \bar{c}c$ production can be effectively removed by $p_T(l), \not{p}_T$, isolation, and $\Delta\phi(l_1 l_2)$ cuts.

(vii) The small $Z, \gamma^* \to \bar{\tau}\tau$ and WW backgrounds are unimportant up to $m_t = 120$ GeV; with an additional $n \geq 2$ jet cut they are substantially smaller than the $\bar{t}t$ signal up to $m_t = 200$ Gev.

(viii) The $Z, \gamma^* \to \bar{\tau}\tau$ background can also be distinguished through many different dynamical distributions.

(ix) The size of a remaining $\bar{t}t$ signal, plus the accompanying jet multiplicity distribution, provide several independent measures of m_t.

(x) The ratios of ee, $e\mu$, $e\tau$, $\mu\mu$, $\mu\tau$, and $\tau\tau$ events provide cross-checks on the $\bar{t}t \to W^- W^+$ origin of an eventual signal.

(xi) Dilepton-$\not{p}_T$ correlations, measured via $\Delta\phi(ll, \not{p}_T)$ and $\Delta p_T(ll, \not{p}_T)$ distributions, offer further cross-checks on the $\bar{t}t \to WW$ origin of a signal and on the value of m_t.

(xii) For an eventual luminosity of 100 pb^{-1}, $\bar{t}t$ dilepton signals can be measured through the entire SM range up to $m_t = 200$ GeV.

In general we conclude that the Tevatron can find the top quark of the standard model; if it does not, new physics will be implied.

ACKNOWLEDGMENTS

This research was supported in part by the University of Wisconsin Research Committee with funds granted by the Wisconsin Alumini Research Foundation, and in part by the U.S. Department of Energy under Contract No. DE-AC02-76ER00881.

[1]For a review, see J. C. Taylor, *Gauge Theories of Weak Interactions* (Cambridge University Press, Cambridge, England, 1976).

[2]V. Barger and S. Pakvasa, Phys. Lett. **81B**, 195 (1979); G. L. Kane and M. Peskin, Nucl. Phys. **B195**, 29 (1982); CLEO Collaboration, A. Bean *et al.*, Phys. Rev. D **35**, 3533 (1987).

[3]JADE Collaboration, W. Bartel *et al.*, Phys. Lett. **146B**, 437 (1984).

[4]TOPAZ Collaboration, M. Yamauchi, in *Proceedings of the XXIV International Conference on High Energy Physics*, Munich, West Germany, 1988, edited by R. Kotthaus and J. Kuhn (Springer, Berlin, 1988).

[5]UA1 Collaboration, C. Albajar *et al.*, Z. Phys. C **37**, 505 (1988); G. Altarelli, M. Diemoz, G. Martinelli, and P. Nason, Nucl. Phys. **B308**, 724 (1988).

[6]U. Amaldi *et al.*, Phys. Rev. D **36**, 1385 (1987); G. Costa *et al.*, Nucl. Phys. **B297**, 244 (1988); J. Ellis and G. Fogli, Phys. Lett. B **213**, 526 (1988).

[7]B. Pendleton and G. G. Ross, Phys. Lett. **98B**, 291 (1981); C. T. Hill, Phys. Rev. D **24**, 691 (1981).

[8]J. Ellis *et al.*, Phys. Lett. B **192**, 201 (1987); Nucl. Phys. **B304**, 205 (1988); I. Bigi and A. Sanda, Phys. Lett. B **194**, 307 (1987); V. Barger *et al.*, *ibid.* **194**, 312 (1987); L. L. Chau and W.-Y. Keung, University of California at Davis Report No. UCD-87-02 (unpublished); D. W. Wu and Z. Zhao, Phys. Rev. Lett. **59**, 1072 (1987); J. Maalampi and M. Roos, Phys.

Lett. B **195**, 489 (1987); H. Harari and Y. Nir, *ibid.* **195**, 586 (1987); J. R. Cudell *et al.*, *ibid.* **196**, 227 (1987); A. Datta *et al.*, *ibid.* **196**, 376 (1987); G. Altarelli and P. Franzini, Z. Phys. C **37**, 271 (1988).

[9]F. Halzen and M. Mursula, Phys. Rev. Lett. **51**, 857 (1983); K. Hikasa, Phys. Rev. D **29**, 1939 (1984); N. Deshpande *et al.*, Phys. Rev. Lett. **54**, 1757 (1985); D. A. Dicus, *et al.*, *ibid.* **55**, 132 (1985); F. Halzen, Phys. Lett. B **182**, 388 (1986); V. Barger *et al.*, *ibid.* **192**, 212 (1987); F. Halzen *et al.*, Phys. Rev. D **37**, 229 (1988); A. D. Martin, W. J. Stirling, and R. G. Roberts, Phys. Lett. B **207**, 205 (1988); R. Ansari *et al.*, *ibid.* B **186**, 440 (1987); C. Albajar *et al.*, *ibid.* B **198**, 271 (1987).

[10]H. Baer, V. Barger, H. Goldberg, and R. J. N. Phillips, Phys. Rev. D **37**, 3152 (1988).

[11]R. Kleiss, A. D. Martin, and W. J. Stirling, Z. Phys. C **39**, 393 (1988).

[12]S. Gupta and D. P. Roy, Z. Phys. C **39**, 417 (1988).

[13]F. Halzen, C. S. Kim, and A. D. Martin, Durham University Report No. DTP/88/34 (unpublished).

[14]P. Nason, S. Dawson, and R. K. Ellis, Nucl. Phys. **B303**, 607 (1988).

[15]D. W. Duke and J. F. Owens, Phys. Rev. D **30**, 49 (1984).

[16]UA1 Collaboration, G. Arnison *et al.*, Europhys. Lett. **1**, 327 (1986); C. Albajar *et al.*, Phys. Lett. B **185**, 233 (1987); UA2 Collaboration, J. A. Appel *et al.*, Z. Phys. C **30**, 1 (1986); CDF Collaboration, S. Errede, in *Proceedings of the XXIV International Conference on High Energy Physics* (Ref. 4).

[17]W. L. van Neerven, J. A. M. Vermaseren, and K. J. F. Gaemers, NIKHEF Report No. H/82-20, 1982 (unpublished); UA1 Collaboration, G. Arnison *et al.*, Phys. Lett. **122B**, 103 (1983). See also J. Smith, W. L. van Neerven, and J. A. M. Vermaseren, Phys. Rev. Lett. **50**, 1738 (1983).

[18]V. Barger, A. D. Martin, and R. J. N. Phillips, Z. Phys. C **21**, 99 (1983).

[19]V. Barger, T. Han, and R. J. N. Phillips, Phys. Rev. D **39**, 146 (1989).

[20]UA2 Collaboration, R. Ansari *et al.*, Phys. Lett. B **186**, 452 (1987).

[21]V. Barger, A. D. Martin, and R. J. N. Phillips, Phys. Lett. **125B**, 339 (1983); **151B**, 463 (1985); Phys. Rev. D **28**, 145 (1983).

[22]Z. Kunszt, Phys. Lett. **145B**, 132 (1984); Z. Kunszt and W. J. Stirling, Phys. Lett. B **171**, 307 (1986).

[23]M. Mangano, Report No. Fermilab-Pub-88/119-T, 1988 (unpublished).

[24]UA1 Collaboration, second paper of Ref. 16.

[25]H. Baer, V. Barger, and R. J. N. Phillips, University of Wisconsin at Madison Report No. MAD/PH/458, 1988 (unpublished).

[26]J. L. Rosner, University of Chicago Report No. EFI 89-02, 1989 (unpublished).

[27]V. Barger and R. J. N. Phillips, Phys. Lett. **143B**, 259 (1984).

[28]R. K. Ellis and J. C. Sexton, Nucl. Phys. **B282**, 642 (1987).

[29]V. Barger, and R. J. N. Phillips, Phys. Rev. Lett. **55**, 2752 (1985).

[30]V. Barger, J. Ohnemus, and R. J. N. Phillips, Int. J. Mod. Phys. A **4**, 617 (1989).

[31]C. Peterson *et al.*, Phys. Rev. D **27**, 105 (1983).

[32]J. Green *et al.*, Phys. Rev. Lett. **51**, 347 (1873).

[33]T. Gottschalk, Nucl. Phys. **B277**, 700 (1986); V. Barger, T. Gottschalk, J. Ohnemus, and R. J. N. Phillips, Phys. Rev. D **32**, 2950 (1985).

[34]V. Barger, T. Han, J. Ohnemus, and D. Zeppenfeld, Phys. Rev. Lett. **62**, 1971 (1989).

[35]R. W. Brown and K. O. Mikaelian, Phys. Rev. D **19**, 922 (1979).

[36]See, e.g., UA1 Collaboration, first paper of Ref. 16.

[37]UA1 Collaboration, G. Arnison *et al.*, Phys. Lett. **122B**, 103 (1983).

[38]UA5 Collaboration, J. G. Rushbrooke, in *Multiparticle Dynamics 1985,* proceedings of the XVIth International Symposium, Kiryat Anavim, Israel, 1985, edited by J. Grunhaus (World Scientific, Singapore, 1985); G. J. Alner *et al.*, Phys. Lett. **167B**, 476 (1986).

[39]R. K. Ellis, G. Martinelli, and R. Petronzio, Nucl. Phys. **B211**, 106 (1983).

[40]H. Baer, V. Barger, and R. J. N. Phillips, Phys. Rev. D **39**, 2809 (1989).

[41]H. Baer, V. Barger, R. J. N. Phillips, and X. Tata, Phys. Lett. B **220**, 303 (1989).